

TWO-DIMENSIONAL DISTRIBUTION OF ICE IN THE LUNAR REGOLITH-MODELING AND INTERPRETATION. D. M. Hurley^{1,5}, D. J. Lawrence^{1,5}, D. B. J. Bussey^{1,5}, R. R. Vondrak^{2,5}, Richard C. Elphic^{3,5}, G. R. Gladstone⁴, ¹JHU Applied Physics Laboratory (dana.hurley@jhuapl.edu), ²NASA Goddard Space Flight Center, ³NASA Ames Research Center, ⁴Southwest Research Institute, ⁵NASA Lunar Science Institute.

Introduction: Analysis of the possibility of water and other volatiles existing in PSRs has a long history (e.g., [1, 2, 3]). The first direct spectroscopic confirmation of their presence came with the impact of the Lunar Crater Observation and Sensing Satellite (LCROSS) into the PSR of Cabeus crater near the lunar south pole [4, 5, 6]. The LCROSS experiment excavated a single sample of one PSR; therefore it lacks the expanse needed to determine the global distribution and quantity of volatiles. However, complementary remote-sensing data that are consistent with ice but cannot confirm its presence can be applied more globally. Different techniques of measuring ice in permanent shadowed regions inherently have different sensitivities, fields of view, and resolution.

Complicating the picture is that volatiles emplaced in lunar polar regions are modified over time by space weathering processes (e.g., [3]). Temperatures are too low for thermal diffusion and sublimation (e.g. [7, 8]); however, volatiles deposited in lunar cold traps are subjected to other destructive mechanisms. It is important to understand the modification processes on several different scales in order to interpret disparate data in a consistent manner.

Model: We have developed a Monte Carlo model similar to [9, 10] that examines the evolution of ice in a permanently shaded region on the Moon [11, 12] and Mercury [13]. Previously, the model simulated the evolution over time of ice with depth in a single vertical column of regolith. We have expanded the model to 2-D to investigate lateral scale lengths of properties of ice [14]. Instead of simulating a single column, we now simulate 2 columns with adjustable lateral separation. We consider impacts and gardening in the area including the pair of columns and allow any impact to affect whichever simulation columns are in the crater radius or ejecta blanket. Correlations between columns provide a look at how features persist in both time and distance.

Each model run here starts with an initial ice layer on the surface that is 10 cm thick and comprised of 100 wt.% water ice. A set of 1000 pairs of columns was run for each lateral separation (1 cm, 10 cm, 1 m, 10 m, 100 m, 1 km). The water concentration as a function of depth for each pair is recorded at times 1, 2, 5, 10, 20, 50, 100, 200, 600, and 1,000 Myr after the ice layer is emplaced.

Results: Because the program is a Monte Carlo program, each run represents a possible scenario, given the inputs to the program. Running a large number of cases with the same program inputs but a different seed to the random generator produces a set of profiles that are representative of what can be expected to occur on the Moon. Taking the average of values generated by the runs with different seeds is the equivalent of computing the large area expectation value. These averages are useful for comparing to large-area footprint data like neutron spectroscopy and FUV spectroscopy. The average weight fraction of ice as a function of time, $f_{ice}(t)$, is fit by the expression $f_{ice}(t \text{ (Myr)}) = f_{ice}(t_0) * (1 - \log(t)/5.74)$. The peak concentration of ice is also pushed below the surface as an ice deposit ages at a rate of 1 mm/Myr.

We examine the heterogeneity as a function of depth and column separation. The surface becomes homogeneous with low water concentration ($f_{ice} < 1$ wt.%) at $t > 20$ Myr. Deviations in the ice layer increase with lateral separation in the 100 Myr case and at later times. Drill cores separated by > 1 m would have very different vertical profiles if for deposits aged > 100 Myr.

Next we determine the probability of retaining a solid chunk of ice (**Fig. 1**). The condition chosen for coherence is that there is a large abundance of ice ($f_{ice} > 0.5$) and that the difference between the abundance in the two columns is small compared to the average value ($|f_{ice}(A) - f_{ice}(B)| < 0.2 < f_{ice}$). The coherence on the ~ 10 cm scale is important for strong radar CPR enhancement; therefore this comparison is done relative to a fixed distance from the center of the Moon rather than distance below the surface. Integrated over the original depths containing ice, the lateral correlation decreases with age. The probability can be fit by the function $P_{ice \text{ chunk}} = 0.904 - \log(t)/3.108$. Detectable ice chunks should remain for ~ 100 Myr. The ice chunks become too small by 1000 Myr.

The next analysis studies the occurrence of dry spots and wet spots. We determine the occurrence rate in which at least one of the two columns is "wet," defined here as ≥ 1 wt. % in the top 1 m (**Fig. 2**). At most ages, the probability is higher with increased lateral separation up to separations of 10 m. Separation beyond 10 m does not increase the probability of finding a wet spot.

Discussion: Lateral coherence disappears quickly on the 20-cm scale according to these simulations. This implies that the ice was deposited in anomalous craters in the north polar region [15] within the last 100 Myr if the features initially began as a 10 cm thick layer. A thicker initial layer would take longer to break apart to the point of losing the radar signature. The model suggests that ice deposits in the larger cold traps including Cabeus, which lack a radar signature, are older than 100 Myr old or started as layers thinner than detectable by radar.

Neutron spectroscopy is able to detect older, diluted deposits that aren't detectable by radar. These older, buried ice deposits have a high degree of heterogeneity in both depth and lateral distribution. Knowledge of a significant surface layer could improve models of neutron leakage used in converting neutron spectra to water abundances. If several ice layers exist and one is on the surface, the standard dry-over-wet model might underestimate the water abundance [16].

Surface frost could appear two ways. First, it could be steadily deposited by migrating volatiles. This case was studied by [11] and is not addressed here. Secondly, volatiles on the surface can represent a partially buried ice layer. As space weathering affects the surface more than it does as depth increases, surface abundances decrease rapidly without additional input. For a surface frost to be present in most permanently shadowed regions, there is likely the addition of volatiles at a steady rate in addition to ice deposited by a comet. The lack of a surface frost signature in Shoemaker [17] and the strong neutron signature are both consistent with an old deposit [18-19]. If stronger surface deposits are found to exist, that might indicate that an ice layer has been exposed recently.

The LCROSS impact excavated a 20-m diameter crater [20]. Timing of the observations of water ice is consistent with the water being derived from a depth of 2-3 m. Furthermore, [18] state that the impact region is enriched in water by a factor of ~ 2 compared to the surrounding area. These simulations suggest that the likelihood of an area of that size being enriched to that degree begins to increase for deposits that are ≥ 1000 Myr old.

An obvious next step in exploring lunar cold traps is to send a lander to drill and analyze the composition and depth distribution of volatiles. The heterogeneity guarantees that variations will exist, and a static lander might have the misfortune of landing in a dry spot. These simulations suggest that a lateral range of ~ 10 m is optimal in the trade between minimizing the probability of probing a dry spot and minimizing mission duration.

References: [1] Urey H. C. (1952) *The Planets, Their Origin and Development*, 17-18. [2] Watson K. et al. (1961) *JGR*, 66, 3033-3045. [3] Arnold J. R. (1979) *JGR*, 84, 5659-5668. [4] Colaprete A. et al. (2010) *Science* 330, 463-468. [5] Gladstone G. R. et al. (2010) *Science* 330, 472-476. [6] Killen R. M. et al. (2010) *GRL*, 37, L23201. [7] Vasavada A. R. et al. (1999) *Icarus*, 141, 179-193. [8] Andreas E. L. (2007) *Icarus* 186, 24-30. [9] Arnold J. R. (1975) *LSC VI*, 2375-2395. [10] Borg J. et al. (1976) *EPSL*, 29, 161-174. [11] Crider D. H. and Vondrak R. R. (2003) *JGR*, 108, 5079. [12] Crider D. H. and Vondrak R. R. (2003) *ASR*, 31, 2293-2298. [13] Crider D. and Killen R. (2005) *GRL*, 32, L12201. [14] Hurley D. M. et al. (submitted) *GRL* [15] Spudis P. D. et al. (2010) *GRL*, 37, L06204. [16] Lawrence D. J. et al. (2011) *JGR*, 116, E01002. [17] Gladstone G. R. et al. (2012) *JGR* 117, E00H04. [18] Feldman W. C. et al. (1998) *Science*, 281, 1496-1500. [19] Mitrofanov I. G. et al. (2010) *Science* 330, 483-486. [20] Schultz P. H. et al. (2010) *Science* 330, 468-472.

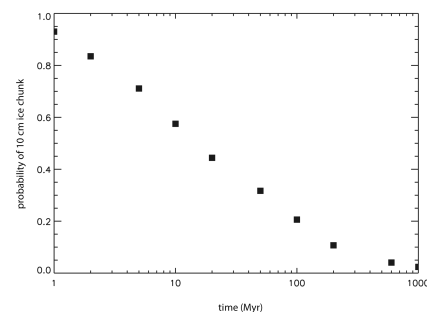


Figure 1. The occurrence rate of ice chunks on the 10 cm size detectable by radar is shown as a function of age of the ice deposit.

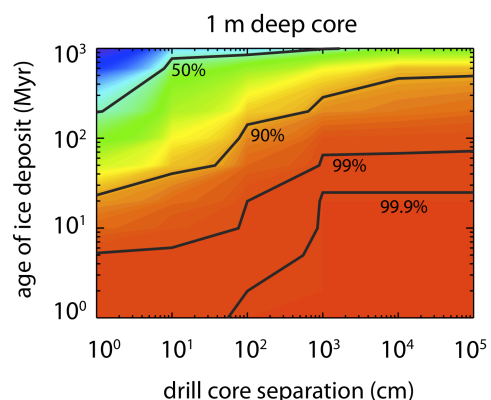


Figure 2. The probability of at least one of the two columns having $> 1\%$ water as a function of age of the deposit and lateral separation.